



1 **Brief communication: Alternation of thaw zones and deep**  
2 **permafrost in the cold climate conditions of the East Siberian**  
3 **Mountains, Suntar-Khayata Range**

4 Robert Sysolyatin<sup>1</sup>, Sergei Serikov<sup>1</sup>, Anatoly Kirillin<sup>1</sup>, Andrey Litovko<sup>1</sup> and Maxim Sivtsev<sup>1</sup>

5 <sup>1</sup>Melnikov Permafrost Institute, Yakutsk, 677000, Russia

6 *Correspondence to:* Robert Sysolyatin (robertseesaw@gmail.com)

7 **Abstract.** The Suntar-Khayata Range include numerous natural phenomena interacting or depending on permafrost  
8 conditions. Here, we examine some patterns of deep permafrost and talik zones on adjacent sites. A 210 m deep  
9 borehole in siltstone bedrock was equipped in July 2010 for temperature monitoring of the topmost 15 m and  
10 measurements of a deep permafrost temperature profile. The temperature curvature in the upper part has a bend which  
11 is consistent with at upper portion justify by climate warming and shows a steady-state linear geothermal profile below  
12 85 m depth with a high geothermal heat flux. A shallow borehole situated at the river floodplain was used to investigate  
13 thaw zones temperature regime. Temperatures down to 6.7 m has been monitored at 5-min intervals during heavy  
14 rainfall and has had quite peculiar way. The thickness of the season freezing layer reach to 5.7 m, moreover ground  
15 temperature increases to 6 °C at 6.7 m depth by groundwater heat transfer. This study provides some new insight on  
16 the permafrost condition at one of the coldest places of Northern Hemisphere.

17 **1 Introductions.**

18 The East Siberian Mountains is one of the largest territory of east Siberia, but at the same time is researching how  
19 frontier permafrost region. On the other hand, the existing unique environmental conditions and natural cryosphere  
20 phenomena (glaciers, aufeis, Pole of Cold Oymyakon and Verkhoyansk e.g.) are interesting for the widespread  
21 scientific community (Lytkin and Galanin, 2016; Makarieva et al., 2022; Takahashi et al., 2011). Despite the  
22 increasing efforts in global permafrost mapping this area has almost no data on direct permafrost measurements and  
23 observations, which would be especially relevant in this data-scarce regions.

24 One of the main permafrost parameter is the permafrost thickness (Osterkamp and Gosink, 1991) which has  
25 considerably importance for paleo-climate reconstruction, hydrogeology description, deposit exploitation etc. The  
26 permafrost temperatures profile is controlled by initial surface temperature, bedrock thermal properties and  
27 geothermal heat flux (Lachenbruch and Marshall, 1986). Most frequently, the data about deep permafrost is acquired  
28 during geological-prospecting works for potential deposits. The expensive costs of deep borehole drilling limit its  
29 acquisition facilities, but in our case, we have access to a deep open borehole on gold ore deposit. In a previous study  
30 we focused on monitoring the active layer temperature regime by a widespread soil-pit network in an area close-by,  
31 but the temperature regime at the layer of zero annual amplitude (ZAA), season freezing layer as well as deep  
32 temperatures profiles have never been presented before (Sysolyatin et al., 2020).

33 Thaw zones (taliks) in cold climate conditions with MAAT down to -12°C is extremely rare (Walvoord and Kurylyk,  
34 2016). Since the heat balance of the subarctic is clearly not cold enough to induce talik formation, groundwater  
35 processes are more often involved. Taliks formed by thermal waters and open taliks (below large rivers) are well  
36 known, but taliks confined to coarse-grained permeable sediments of riverbanks are poorly studied (Makarieva et al.,



37 2019). Floodplain sediments can accumulate water during the warm period and gradually empty in the winter  
38 (Mikhailov, 2015). The occurrence of such taliks forms a favorable environment for the growth thermophilic plants  
39 out of their species range – e.g., poplar, willow shrub formation.

40 In this brief communication, we present the thermal regime of typical permafrost and talik sites at the Suntar-Khayata  
41 Range. The successful embedding of a shallow borehole allows to examine the active layer temperature evolution in  
42 a floodplain talik for the first time. We aim to: 1) describe the typical permafrost conditions by possess data and  
43 discuss the present temperature changes 2) infer the possible extent of talik zones, discuss the origin of their formation  
44 and show the impact of heavy rainfall to ground temperature regime and slope stability. This study presents the general  
45 permafrost conditions and discusses possible ways to improve the permafrost mapping of the East Siberian Mountains.

## 46 **2 Study area.**

47 The Suntar-Khayata Range is located at the southern boundary of the East Siberian Mountains and serves as a  
48 watershed between Aldan and Indigirka River basins (Fig. 1). At altitudes between 2000 m asl and 2959 m asl a glacial  
49 area is persisting, representing largest of present glaciation in Siberia – with about 195 glaciers cover 163 km<sup>2</sup>  
50 (Ananicheva et al., 2010). The study area is represented by alpine relief with the height of the peaks from 1550 to  
51 2031 m asl. The shallow borehole is located at the valley basin of Vostochnaya Khandyga River at 850 m asl (Fig.  
52 1d), and the deep borehole is located in the narrow V-shaped valley Vostochnaya Khandyga tributary at 1100 m asl  
53 altitude (Fig. 1c). Late Paleozoic sandstone, siltstone and clay slate are prevalent bedrocks of the mountain rock,  
54 whereas the valley sediments consist of coarse-grained alluvium strata (Sokolov et al., 2015). Rock glaciers are  
55 widespread at the foot and middle part of the mountain slopes and has widespread distribution (Lytkin and Galanin,  
56 2016). and boulders can reach up to 3 m in diameter.

57 The climate conditions recorded at a weather station 43 km away from to east of the study site, situated at 1288 m asl.  
58 The MAAT ranges from -15.3°C to -11.2°C, average precipitation is about 280 mm and maximum annual snow  
59 thickness vary from the 16 to 60 cm for the 1966-2018 period. Direct air temperature observation around the borehole  
60 at the floodplain shown the existence of winter temperature inversion at altitudes between 800 and 1400 m asl  
61 (Sysolyatin et al., 2020). The flora is not very diverse. Dwarf Siberian pine is occupying the top part of slopes between  
62 1400 and 1600 m asl and able to accumulate significant snow cover. Siberian larch is growing on gentle and steep  
63 slopes, flat surfaces reflecting the most severe permafrost conditions. The poplars have a limited extent, adjacent to  
64 the riverbank.

65 According to our soil-pit monitoring network (Sysolyatin et al., 2020), the mean annual ground temperature ranges  
66 from -1.1 to -10.6°C at 1 m depth, active layer vary from 0.5 to 2.7 m and mean ground surface temperature can drop  
67 to -31°C. No direct observation of precipitation or snow thickness are available for the study area, but its influence is  
68 obviously significant. For instance, in 2021 anomalous heavy rains gave rise to numerous debris flows and the  
69 appearance of debris avalanches as well as an abrupt change in the talik temperature regime (Supplementary material,  
70 Fig. 3).

## 71 **3 Materials and method**

72 The deep borehole was drilled for prospecting of the orogenic gold deposit prospecting by a geological company in  
73 1991. Organic mat is almost absent and soil thickness does not exceed 0.5-0.8 m. Core samples (with marked depths  
74 interval) were stocked close to the drilling site, where 4 samples have been collected for laboratory studies. In 2010  
75 the sintered ice plug in the topmost 5 m was redrilled for establishing a temperature monitoring site. In 2020,



76 temperature measurements were made at intervals of 5 m for depths of 20 to 150 m and 10 m for depths between 150  
77 and 210 m using a movable high-precision negative temperature coefficient thermistor and multiconductor cable. To  
78 reduce the impact of convection, the hole was plugged by dense material.

79 The shallow borehole was drilled using a wheeled drilling rig in gravel alluvium sediments without core sampling.  
80 The hole was cased with a PVC pipe with inner diameter of 20 mm and the sensors were inserted at 1, 3, 5 and 6.7 m  
81 depths. The space around the casing was filled by sand and well cutting. The first attempt to drill a borehole in the  
82 floodplain was reaching to a depth of 12 m, but a failure of drilling tools halted the process. At end of July the stratum  
83 was relatively dry.

84 Ground temperatures were monitored continuously within the shallow and deep borehole down to 6.7 and 15 m for  
85 one and 9 years, respectively. Measurements were made every 4 h with TMC50-HD thermistors that were attached to  
86 four-channel Onset HOBO data loggers (U12-008 model). Air and ground surface temperatures (2 cm depth) were  
87 acquired for the shallow borehole site using a 2-channel data logger (U23-003). These logger systems have an accuracy  
88 of  $\pm 0.25^\circ\text{C}$  or better and an operation range of  $-40$  to  $100^\circ\text{C}$ . Since the sensors installed in the deep borehole at 5 and  
89 15 m, we report the mean annual ground temperature determine the offset of heat wave penetration from surface. In  
90 accordance with local climatic conditions and thermal properties of the bedrock, to account for an equal seasonal  
91 cycle, MAGT was calculated for the periods September-August and January-December for depths of 5 and 15 m,  
92 respectively. For the shallow boreholes, the data presented for the high-frequency logging period (every 5 min) from  
93 31 July to 8 September are used trace the impact of heavy rain infiltration events on the subsurface thermal regime.

## 94 **4 Result**

### 95 *4.1 Permafrost temperature evolution*

96 At the V-valley site, only two of four sensors (5 and 15 m) have useful and reliable data for analysis (Fig 2a and b).  
97 The ground temperatures below  $0^\circ\text{C}$  were recorded for the whole monitoring period at 5 m depth. The observed  
98 average MAGT is  $-4.25^\circ\text{C}$  for both depths. The ground temperature evolution show a sinusoidal pattern with smooth  
99 drifting following the changing climate condition. At 5- and 15 m depth, the amplitude ranges from 6.2 to 0.6  $^\circ\text{C}$ ,  
100 respectively, for the whole measurement period. The fluctuations of mean annual ground temperature did not exceed  
101  $0.61^\circ\text{C}$  at 5 m and  $0.26^\circ\text{C}$  at 15 m. The warming trend that has been highlighted for the 2010 to 2015 period was  
102 changing to equivalent cooling until 2019 at both depths. In accordance with the results presented, the ZAA depth  
103 might vary from 10.9 to 13.9 for a thermal diffusivity of around  $1.21\text{-}1.96 \times 10^{-6} \text{ m}^2 \text{ s}^{-1}$  by core samples. However, as  
104 far as the temperature altering should not up over to  $0.1^\circ\text{C}$  by annual period, the ZAA layer has been exceed 15 m  
105 depth.

### 106 *4.2 Permafrost thickness and thermal conditions*

107 The permafrost thickness observed by these direct measurements does not exceed 205-210 m in the deep borehole at  
108 V-valley. A detailed temperature profile is presented in Fig. 2c. Below the assumed depth of ZAA (20 m), the  
109 permafrost temperature increases downwards with a gradient ranging from 0.01 to  $0.038^\circ\text{C}^{-1} \text{ m}$ . From the whole  
110 temperature curve the mean gradient was calculated as  $0.0214^\circ\text{C}^{-1} \text{ m}$ . The initial surface temperature ( $T_0 = -5.25^\circ\text{C}$ ) is  
111 obtained by best-fit linear extrapolation from a depth interval of 85-160 m due to the uniform value of the gradient  
112 (Lachenbruch and Marshall, 1986). The values for the temperature anomaly (offset value from linear fit) at 20 m ( $A_{20}$ )  
113 and 40 m ( $A_{40}$ ), were calculated as  $0.70$  and  $0.39^\circ\text{C}$ , respectively.



#### 114 4.3 Talik temperature regime

115 A simple geomorphology sketch of the shallow borehole site is present in Figure 3a and an annual and monthly  
116 temperature-time series for the floodplain site are shown in Figure 3b and c, respectively. The pattern of the 1 m depth  
117 temperature evolution is consistent with the air and surface temperature evolution. Temperatures ranged from -6.3 to  
118 6.6 °C and from -13.7 to 20.7 °C, respectively. Surprisingly, the temperature variation at 3m depth has been smaller  
119 than for the sensors below, just from -2 to 1.6 °C. Refreezing at 3 m depth began at the end of January and the zero-  
120 curtain period is present from approximately the end of June to September, dividing the floodplain (overburden)  
121 sediments into to 3 zones – upper active layer, intermediate frozen layer and bottom permanent talik. The spike in  
122 Figure 3c is related to percolation of warm rainwater to 3 m depth, probably through casing tube. The most peculiar  
123 temperature behavior is found for the 5 and 6.7 m depth sensors, which is surely related to heat advection of ground  
124 water movement. Patterns of temperature changes at 5 m depth are more linear, whereas at 6.7 m it is more exponential.  
125 The maximum absolute temperature ranged between 4.4 °C (5 m) and 7.7 °C (6.7 m), while minimum temperatures  
126 oscillated between -0.2 °C (5 m) and 0.3 °C (6.7 m). The ground at a depth of 5 m remained unfrozen for more than  
127 75% of the time of the year. In an isopleth plot the thaw zone appears below to 5.7 m and obviously continuous  
128 downward (Fig 3b). At an air temperature of -9.9 °C and MAGST of -1.8 °C the MAGT for the observation period  
129 (almost a year) is -1.1, -0.1, 1.1, 1.8 °C for depths of 1, 3, 5 and 6.7 m, respectively.

#### 130 5 Discussion

131 Permafrost thickness is one of the major components of the cryosphere and has a close relation to geothermal heat  
132 flux. According to Balobaev (Balobaev et al., 1985) the Suntar-Khayat Range is characterised by high values of  
133 geothermal heat flux up to 0.08-0.10 Wm<sup>-2</sup>, usually concentrating under narrow V-shaped valleys. Through numerous  
134 geothermal measurements at the next orogenic gold deposits (Nezhdaninskoye) specific patterns of thermal conditions  
135 were determined. Thus, the angle of inclination of the surface reduces the geothermal heat flux according to the  
136 equation:

$$137 \quad q = q_0 \cos \alpha \quad (1)$$

138 where  $q$  – calculated geothermal heat flux;  $q_0$  – initial geothermal heat flux,  $\alpha$  – slope angle.

139 The interaction between altitude and surface temperature has also been presented in previous studies and might  
140 decrease MAGST to -6.5°C at 1800 m asl mountain peaks (Sysolyatin et al., 2020). As mentioned above, MAGT at 5  
141 m depth have rather similar value to the ZAA temperature. By the steady-state equation (2) and expect the decrease  
142 of the ZAA temperature upon upward height, the permafrost thickness was calculated (Table 1) (Carslow and Jager,  
143 1959; Guglielmin et al., 2011). By corn samples, bedrock effective thermal conductivity is 2.41 Wm<sup>-1</sup> K<sup>-1</sup> and  $q_0 =$   
144 0.052 Wm<sup>-2</sup> in permafrost body at base altitude surface level – 1100 m According to the orographic configuration of  
145 the study area, the permafrost thickness at local peaks 2000 m asl can reach to ~ 500 m.

$$146 \quad Z = T * \frac{\lambda}{q} + ZAA \quad (2)$$

147 where,  $Z$  – estimated permafrost thickness, m;  $T$  – temperature at the ZAA depth, °C;  $\lambda$  – effective thermal  
148 conductivity, Wm<sup>-1</sup> °C<sup>-1</sup>;  $q$  – geothermal heat flux in permafrost Wm<sup>-2</sup> (from equation 1).

149 Extrapolation of the linear portion of temperature curve to the surface result in significant differences to the current  
150 temperature curve from the initial MAGST features (Lachenbruch and Marshall, 1986). Two variants of changes are



151 considered, a temperature change at the surface and a temperature change at the ZAA. For instance, assuming thermal  
152 diffusivity is  $1.6 \times 10^{-6} \text{ m}^2 \text{ s}^{-1}$ , the surface temperature shift around  $1.4 \text{ }^\circ\text{C}$  would be ongoing from 22 to 81-year respect  
153 to step, linear or exponential way of changes. When the temperature shifts by  $0.7^\circ\text{C}$  at the ZAA, the response time  
154 will expand to a range of 19 to 90 years. With the available data about the rate of air temperature change at the closest  
155 weather station, the second variant is the most plausible. It should be noted that the snow cover can change the surface  
156 temperature by more than  $5 \text{ }^\circ\text{C}$  (Gisnas et al., 2014), which is much larger than the air temperature change over the  
157 last 80 years (IPCC, 2014).

158 As mentioned above, the talik appearance can only be caused by the thermal influence of superficial or ground water  
159 in the cold environments of northeastern Siberia. The absence of permafrost under large rivers and in the areas adjacent  
160 to hot springs is well-known. Nevertheless, in our case, where the distance from the main stream exceeds 1 km, the  
161 presence of the talik was not assumed before. The reason for the existence of the talik is ambiguous. (i) One possibility  
162 is the migration of rainwater infiltrating through the "windows" of the rock glaciers on the adjacent slope. The timing  
163 of the thermal impact of rainfall is clearly evident on the temperature graph at a depth of 1 m; these spikes have been  
164 well explained before (Hinkel et al., 2001). (ii) The divergent temperature response at depths of 5 and 6.7 m is difficult  
165 to explain, perhaps it may be related to the interaction of rainfall with the permafrost occurrence at depth. It could also  
166 have been due to a delay in the influence of groundwater supply from the river. However, the response time is largely  
167 consistent with the first hypothesis. The influence of groundwater from the river when considering the thawing cycle  
168 is certain. On the isopleth plot it is clearly shown that the temperature at the depth of 5 and 6.7 m begins to increase  
169 earlier than at a depth of 3 m, which means the proximity to the groundwater is accelerating warming for the coarse-  
170 grained sediments. To solve this issue, it would be necessary to install additional piezometric and temperature  
171 monitoring sites, as well as to carry out temperature measurements of the river water.

172 The features of floodplain taliks for Kolyma region are considered rather recently (Mikhailov, 2015). It is noted as the  
173 crucial reason for the formation of the winter river flow. Floodplain taliks of the region are capable to accumulate  
174 huge amounts of water and gradually return it back to the river during low-flow cold season. The main influencing  
175 factors are the slope of the river floodplain and the permeability of the sediments. Probably the reason for the  
176 appearance of such a large talik is just related to the site-specific conditions of the study area. A sufficiently reliable  
177 marker may be the areal of poplar trees, tending to warmer environments. However, in our case, at the drilling site the  
178 vegetation was represented by mosses and larch that is more typical for permafrost landscapes.

179 An increase in liquid precipitation, along with increase in air temperature, is one of the most obvious consequences  
180 of global warming (Savelieva et al., 2000; Yang et al., 2005). For the permafrost zone, heavy rainfall often acts as a  
181 trigger for geomorphological processes (Borgatti and Soldati, 2013). The effect of heavy rainfalls on permafrost is  
182 most pronounced for the mountainous areas.

183 The behavior of the upper part of the permafrost during flooding rains, creates reasons for the activation of slope  
184 processes. Heavy rains at the end of August 2021 were the trigger for 7 large landslides on a 5 km section of the  
185 Kolyma highway, temporarily stopping traffic (Supplementary material). The high concentration of landslides on this  
186 section is explained by the aspect and angle of the slope, creating favorable conditions for an increase of the active  
187 layer. Abrupt and abundant saturation with rainwater led to critical weighting of soil material, after which the stability  
188 of the slope has been disrupted. Landslide processes were also observed everywhere during field investigations in  
189 other areas with a lower inclination and northern and eastern aspects. Descriptions of such scenarios are given in many



190 sources, but the detailed process for regions of northeastern Siberia is poorly understood at this time (Frauenfelder et  
191 al., 2018; Geertsema et al., 2006; Gruber and Haeberli, 2007).

## 192 **6 Conclusion**

193 This study provides insight into thermal patterns of permafrost and thaw zones (talik) that can be valuable for future  
194 studies of the East Siberian Mountains. Permafrost is almost continuously distributed with a thickness reach to 500  
195 m. By direct measurements and exploration we obtained thermal properties and determined the permafrost temperature  
196 trend. Due to the successful location of the borehole and high-frequency measurements during rare heavy rains in  
197 August 2021, unusually high values of daily precipitation were recorded in the Suntar Khayata Mountains  
198 (Verkhoyansk Ridge, Siberia). Due to the abundance of liquid precipitation, peculiarities of the configuration of  
199 permafrost and thaw zones, as well as site morphology, the temperature regime of soils has a peculiar feature down to  
200 a depth of 6.7 m. The size of the talik zone can be very significant, which must be taken into account in mapping,  
201 design and modeling. A wide range of multidisciplinary research is required to improve the understanding of  
202 permafrost conditions in this area.

### 203 *Data availability*

204 *The data are available from the authors upon request.*

### 205 *Supplement*

206 *Debris landslides evidence are added at supplement*

### 207 *Author contributions*

### 208 *Competing interests*

209 The authors declare that they have no conflict of interest.

## 210 **Acknowledgments**

211 This study has been funded by Republic of Sakha (Yakutia) and Russian Science Foundation (project N 22-27-20073).

## 212 **References**

- 213 Ananicheva, M. D., Krenke, A. N. and Barry, R. G.: The Northeast Asia mountain glaciers in the near future by  
214 AOGCM scenarios, *Cryosph.*, 4(4), 435–445, doi:10.5194/tc-4-435-2010, 2010.
- 215 Balobaev, V. T., Devyatkin, V. N., Gavriliev, R. I. and Rusakov, V. G.: About geothermophysical researching of  
216 mineral deposits at north-east region, *Geol. Geol. Explor.*, 5, 36–37, 1985.
- 217 Borgatti, L. and Soldati, M.: 7.30 Hillslope Processes and Climate Change, in *Treatise on Geomorphology*, pp. 306–  
218 319, Elsevier., 2013.
- 219 Carslow, H. S. and Jager, J. C.: *Conduction of Heat in Solids*, Oxford University Press: New York., 1959.
- 220 Frauenfelder, R., Isaksen, K., Lato, M. J. and Noetzli, J.: Ground thermal and geomechanical conditions in a  
221 permafrost-affected high-latitude rock avalanche site (Polvartinden, northern Norway), *Cryosph.*, 12(4), 1531–1550,  
222 doi:10.5194/tc-12-1531-2018, 2018.



- 223 Geertsema, M., Clague, J. J., Schwab, J. W. and Evans, S. G.: An overview of recent large catastrophic landslides in  
224 northern British Columbia, Canada, *Eng. Geol.*, 83(1–3), 120–143, doi:10.1016/j.enggeo.2005.06.028, 2006.
- 225 Gisas, K., Westermann, S., Schuler, T. V., Litherland, T., Isaksen, K., Boike, J. and Eitzelmüller, B.: A statistical  
226 approach to represent small-scale variability of permafrost temperatures due to snow cover, *Cryosphere*, 8(6), 2063–  
227 2074, doi:10.5194/tc-8-2063-2014, 2014.
- 228 Gruber, S. and Haeblerli, W.: Permafrost in steep bedrock slopes and its temperature-related destabilization  
229 following climate change, *J. Geophys. Res. Surf.*, 112(F2), doi:10.1029/2006jf000547, 2007.
- 230 Guglielmin, M., Baks, M. R., Adlam, L. S. and Baio, F.: Permafrost Thermal Regime from Two 30-m Deep  
231 Boreholes in Southern Victoria Land, Antarctica, *Permafrost. Periglac. Process.*, 22(2), 129–139, doi:10.1002/ppp.715,  
232 2011.
- 233 Hinkel, K. M., Paetzold, F., Nelson, F. E. and Bockheim, J. G.: Patterns of soil temperature and moisture in the  
234 active layer and upper permafrost at Barrow, Alaska: 1993–1999, *Glob. Planet. Change*, 29(3–4), 293–309,  
235 doi:10.1016/S0921-8181(01)00096-0, 2001.
- 236 IPCC: Climate Change 2014, in Synthesis Report, Contribution of Working Groups I, II and III to the Fifth  
237 Assessment Report of the Intergovernmental Panel on Climate Change, p. 151, Geneva, Switzerland., 2014.
- 238 Lachenbruch, A. H. and Marshall, B. V.: Changing Climate: Geothermal Evidence from Permafrost in the Alaskan  
239 Arctic, *Science (80-. )*, 234(4777), 689–696, doi:10.1126/science.234.4777.689, 1986.
- 240 Lytkin, V. M. and Galanin, A. A.: Rock glaciers in the Suntar-Khayata Range, *Ice Snow*, 56(4), 511–524,  
241 doi:10.15356/2076-6734-2016-4-511-524, 2016.
- 242 Makarieva, O., Nesterova, N., Post, D. A., Sherstyukov, A. and Lebedeva, L.: Warming temperatures are impacting  
243 the hydrometeorological regime of Russian rivers in the zone of continuous permafrost, *Cryosph.*, 13(6), 1635–  
244 1659, doi:10.5194/tc-13-1635-2019, 2019.
- 245 Makarieva, O., Nesterova, N., Shikhov, A., Zemlianskova, A., Luo, D., Ostashov, A. and Alexeev, V.: Giant  
246 Aufeis—Unknown Glaciation in North-Eastern Eurasia According to Landsat Images 2013–2019, *Remote Sens.*,  
247 14(17), 4248, doi:10.3390/rs14174248, 2022.
- 248 Mikhailov, V. M.: Geographical regularities of distribution of floodplain taliks, *Izv. Ross. Akad. Nauk. Seriya*  
249 *Geogr.*, (1), 65, doi:10.15356/0373-2444-2014-1-65-74, 2015.
- 250 Osterkamp, T. E. and Gosink, J. P.: Variations in permafrost thickness in response to changes in paleoclimate, *J.*  
251 *Geophys. Res. Solid Earth*, 96(B3), 4423–4434, doi:10.1029/90JB02492, 1991.
- 252 Savelieva, N. ., Semiletov, I. ., Vasilevskaya, L. . and Pugach, S. .: A climate shift in seasonal values of  
253 meteorological and hydrological parameters for Northeastern Asia, *Prog. Oceanogr.*, 47(2–4), 279–297,  
254 doi:10.1016/S0079-6611(00)00039-2, 2000.
- 255 Sokolov, S. D., Tuchkova, M. I., Ganelin, A. V., Bondarenko, G. E. and Layer, P.: Tectonics of the South Anyui  
256 Suture, Northeastern Asia, *Geotectonics*, 49(1), 3–26, doi:10.1134/S0016852115010057, 2015.
- 257 Solsolyatin, R., Serikov, S., Zheleznyak, M., Tikhonravova, Y., Skachkov, Y., Zhizhin, V. and Rojina, M.:



258 Temperature monitoring from 2012 to 2019 in central part of Suntar-Khayat Ridge, Russia, *J. Mt. Sci.*, 17(10),  
259 2321–2338, doi:10.1007/s11629-020-6175-3, 2020.

260 Takahashi, S., Sugiura, K., Kameda, T., Enomoto, H., Kononov, Y., Ananicheva, M. D. and Kapustin, G.: Response  
261 of glaciers in the Suntar–Khayata range, eastern Siberia, to climate change, *Ann. Glaciol.*, 52(58), 185–192,  
262 doi:10.3189/172756411797252086, 2011.

263 Walvoord, M. A. and Kurylyk, B. L.: Hydrologic Impacts of Thawing Permafrost-A Review, *Vadose Zo. J.*, 15(6),  
264 vzj2016.01.0010, doi:10.2136/vzj2016.01.0010, 2016.

265 Yang, D., Kane, D., Zhang, Z., Legates, D. and Goodison, B.: Bias corrections of long-term (1973-2004) daily  
266 precipitation data over the northern regions, *Geophys. Res. Lett.*, 32(19), n/a-n/a, doi:10.1029/2005GL024057,  
267 2005.

268

269

270

271

272

273

274

275

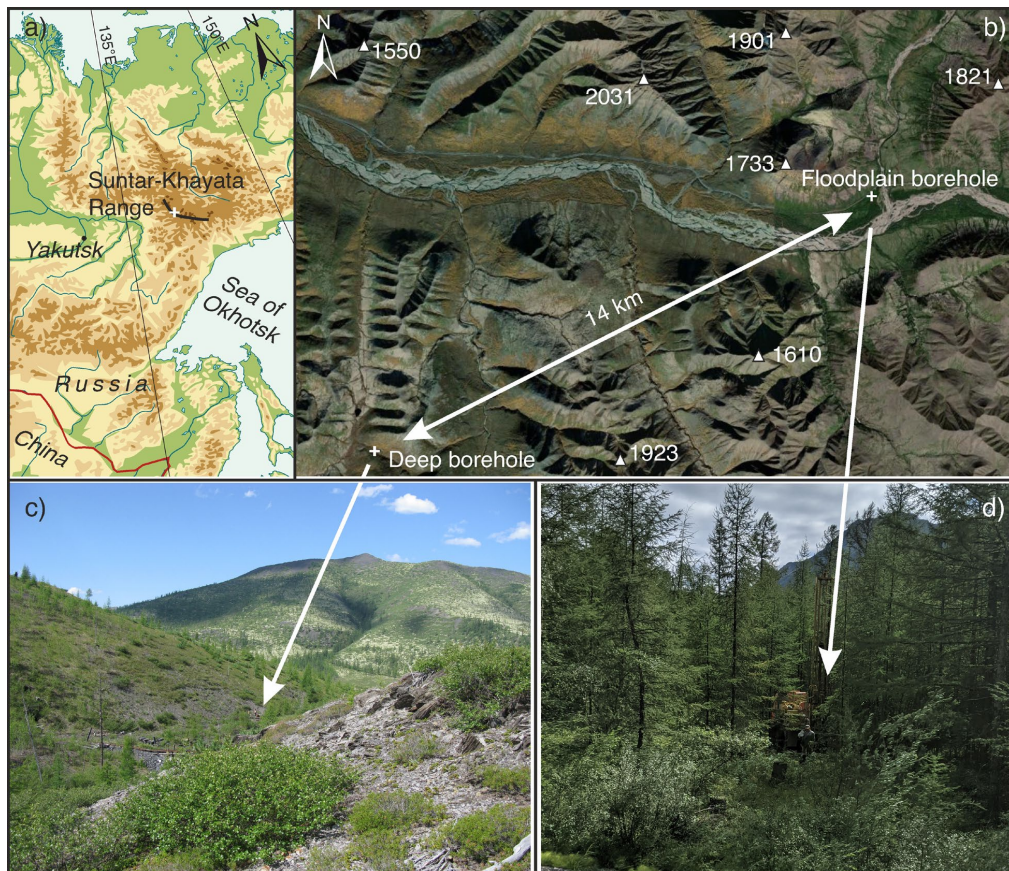
276

277

278

279

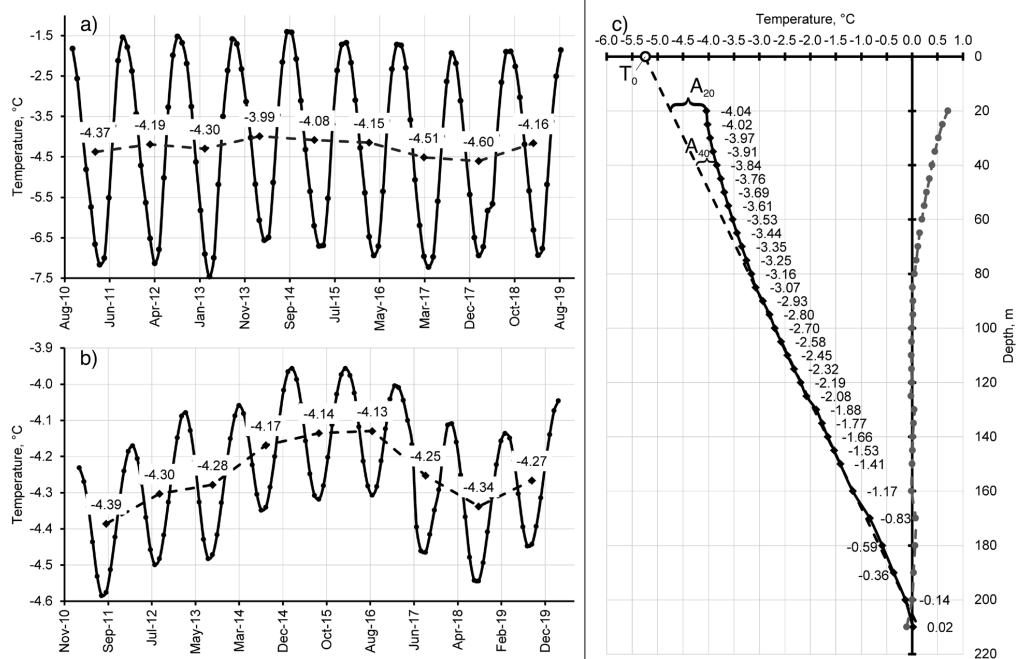




280

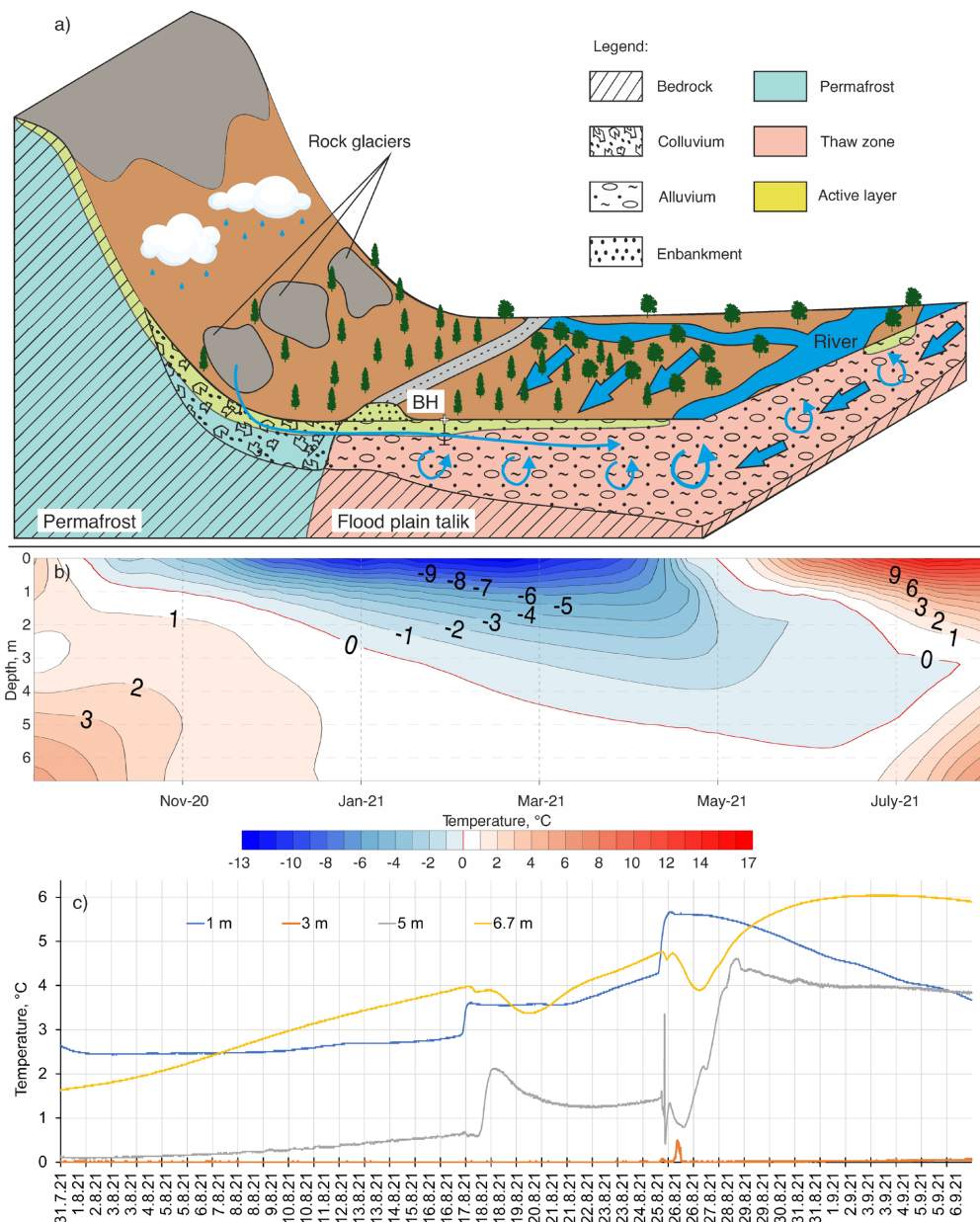
281 **Figure 1.** Study area description and picture of sites environment. In (a) a modified physical map of the location of the study  
282 area in eastern Siberia is shown (Map source: © GEOATLAS 1998). (b) MAXAR image of Vostochnaya Khandyga basin  
283 with altitudes of peaks. (c) Deep borehole site at V-shaping valley. (d) Shallow borehole site at river plain.

284



285

286 **Figure 2: Thermal regime of permafrost conditions in the deep borehole. Mean monthly and annual ground temperature**  
287 **evolution at 5 m (a) and 15 m (b) depth. (c) Temperature profile (solid line), best linear-fit (dashed line) and current offset**  
288 **from extrapolated temperature (dotted line).**



289

290 **Figure 3: (a) The scenario of ground water flow of the floodplain talik. (b) Annual ground temperature evolution and (c)**  
 291 **temperature fluctuation at a heavy rain event.**

292

293

294

295



296

Table 1

297 Permafrost thickness based on the assumption that MAGT and permafrost heat flow are decreasing under step-up of  
298 peaks height.

Peak altitude, m	Slope inclination ( $\alpha$ ), grad	Cos $\alpha$	Temperature at ZAA (20 m depth), °C	q, Wm <sup>-2</sup> ,	Permafrost thickness, m
1550	24.2	0.912	-5.5	0.047	298
1600	26.6	0.894	-5.7	0.047	314
1700	31.0	0.857	-6.0	0.045	343
1800	35.0	0.819	-6.5	0.043	386
1900	38.7	0.781	-7.0	0.041	434
2000	42.0	0.743	-7.5	0.039	486

299